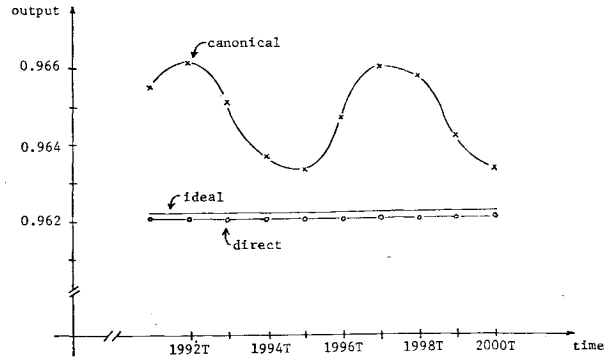

Fig. 3 Step responses for system.

tain T represent ideal delays of T sec. To simplify analysis, only one quantizer Q is considered. The open-loop system transfer function is

$$D(z)G(z) = \left[\frac{z - 0.3545}{z - 0.0499}\right]\left[\frac{0.75(z + 0.5)}{(z - 0.9)(z - 0.7)}\right] \quad (7)$$

where $D(z)$ is the transfer function of the controller, and $G(z)$ is the transfer function of the plant. The digital controller, when realized in the manner shown in Fig. 1, is said to be realized by the canonical programing form. The state equations for this system are

$$\mathbf{x}(k+1) = \begin{bmatrix} 0 & 1 & 0 \\ -1.005 & 0.85 & 0.2285 \\ -0.5Q & -Q & 0.3545Q \end{bmatrix} \mathbf{x}(k) + \begin{bmatrix} 0 \\ 0.75 \\ Q \end{bmatrix} u(k) \quad (8)$$

In Eq. (8), Q is the nonlinear gain of the quantizer. In Fig. 1, if $x_3(k)$ becomes constant, Eq. (8) may be written as

$$\mathbf{x}(k+1) = \begin{bmatrix} 0 & 1 & 0 \\ -1.005 & 0.85 & 0 \\ 0 & 0 & 0 \end{bmatrix} \mathbf{x}(k) + \begin{bmatrix} 0 \\ 0.75 \\ 0 \end{bmatrix} u(k) + \begin{bmatrix} 0 & 0 & 0 \\ 0 & 0 & 0.2285 \\ 0 & 0 & 1 \end{bmatrix} \mathbf{x} \quad (9)$$

Equation (9) represents an unstable system; thus the digital control system will contain oscillations.

These effects may also be viewed in terms of the poles and zeros of the controller. When $x_3(k)$ becomes constant over several sampling instants, no information concerning the changes that occur within the system is transmitted through the quantizer, and thus both the pole and the zero of the controller are in effect removed from the system. The system is unstable for this case.

(Consider the same system, with the controller realized by a different procedure. The diagram of this programing procedure is shown in Fig. 2, and is called the direct programing form.) For this case, if the quantizer transmits no information on changes within the system, only the pole of the controller is removed. The resultant system is stable, and no low-amplitude oscillations will be present.

Figure 3 illustrates the system unit-step response for the two programing forms, after approximately 2000 sampling instants. Floating-point arithmetic was used in the controller, with three bits in the fraction. An expanded scale is used to clearly illustrate the oscillations. The ideal response of Fig. 3 is the system response with no quantization present. These results were obtained from a digital simulation.

Conclusions

A cause of low-amplitude oscillations in digital control systems is presented. It is illustrated through an example that the oscillations are related to the programing form used in the digital controller. This relationship can be explained from the effect of the quantizer on the poles and zeros of the digital controller, when the quantizer is transmitting no information.

Reference

[1] Bertram, J. E., "The effect of quantization in sampled-feedback systems," *AIEE Transactions on Applications and Industry*, Vol. 77, 1958, pp. 177–182.

Viscous Slipstream Flow Downstream of a Centerline Mach Reflection

LLOYD H. BACK* AND ROBERT F. CUFFEL†
Jet Propulsion Laboratory, Pasadena, Calif.

Nomenclature

b = shear layer half-width
l = shock stem height, 0.34 in.
M = Mach number
p = static pressure
p_t' = Pitot pressure
r = radial distance
R = gas constant
z = axial distance
T = temperature
u = axial velocity
v' = transverse turbulent velocity, $\overline{(v'^2)}^{1/2}$
γ = specific heat ratio
μ = viscosity
ρ = density
ψ = stream function

Subscripts

ℓ = centerline condition
0 = reservoir condition
s = condition at edge of slipstream
t = stagnation condition
1 = condition upstream of shock stem
2 = condition just downstream of shock stem

Introduction

AN important aspect of supersonic flows with shock waves is the reflections of these waves at boundaries such as along centerlines, along surfaces, and along free jet extremities. The first of these interactions is considered herein for a situation where the reflection from the centerline in an axisymmetric flow is through a shock stem (Mach reflection). The wave pattern is depicted in Fig. 1. The incident shock wave is S_i, the reflected shock wave is S_r, and the stem shock wave is S_n; a slipstream emanates from the triple shock wave intersection T. The purpose of this investigation is to determine the mean structure of the viscous flowfield downstream of the intersection from Pitot and static pressure probe measurements. There is virtually no experimental information available on the structure of such a shear flow and on the size of the subsonic flow region that is imbedded in the supersonic flow.

This region is of interest because such a shock wave reflection is often found in supersonic flows. Examples are 1) inside of channels where shock waves generated upstream in the flow by compressive turning subsequently undergo reflections from the centerline and the boundary layer along the

Received April 30, 1971; revision received June 4, 1971. This work presents the results of one phase of research carried out in the Propulsion Research and Advanced Concepts Section of the Jet Propulsion Laboratory, California Institute of Technology, under Contract NAS7-100, sponsored by NASA.

Index category: Viscous Nonboundary-Layer Flows.

* Member Technical Staff. Associate Fellow AIAA.
† Member Technical Staff. Member AIAA.

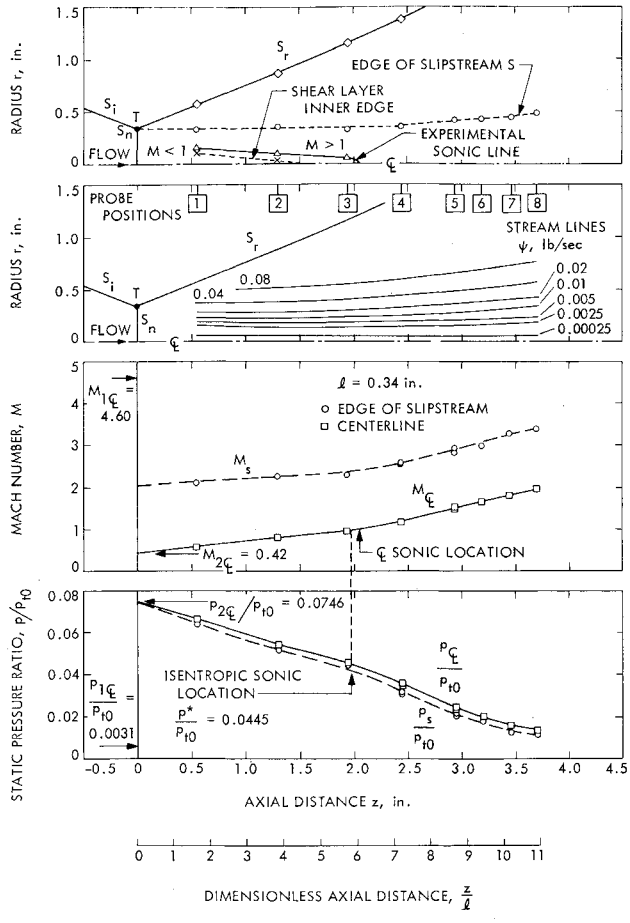

Fig. 1 Centerline Mach reflection—Mach numbers and static pressures along the centerline and edge of the slipstream.

wall[1]; 2) in supersonic exhaust jets from nozzles when the flow is either underexpanded and a barrel shock wave is reflected off the centerline through a Mach disk (shock stem, e.g., see the survey in Ref. 2) or overexpanded and the oblique shock wave that compresses the flow can be reflected off the centerline through a stem shock wave[3]; and 3) in overexpanded supersonic nozzle flow when shock-induced flow separation occurs.[4,5] The present investigation is also related to the generation of noise in supersonic jets where slipstream shear layers produce turbulence and consequently noise. It appears that the most intense noise generated in a supersonic jet originates in the region where the flow becomes subsonic along the centerline.[6]

Measurements and Probes

The measurements were made in air flowing through an axisymmetric supersonic diffuser. The stagnation-pressure upstream of the nozzle which preceded the diffuser p_{to} was 100 psia and the stagnation temperature was 535°R. The Mach number of the expanded flow was 4.60 upstream of the centerline Mach reflection. The shear layer flow downstream of the Mach reflection was believed to be turbulent since the Reynolds number based on the shock stem height l, descriptive of the shear layer thickness, was relatively large, i.e., $\rho_2 u_2 l/\mu_2 = 4.2 \times 10^4$.

Surveys across the flow were made at a number of axial locations with a flattened Pitot tube which had a tip height of 0.005 in. and with static pressure probes. The static pressure probes had blunted conical tips and had an outside diameter of 0.020 in. A static pressure hole, 0.008-in. diam, was located on the side of the probes a distance of either 10 or 15 probe diameters from the tip. The static pressures measured with these probes were within 2% of the local static pressure in the supersonic region,[7] and they were essentially the local static pressure in the subsonic region. There is less certainty in the static pressure probe readings in the transonic region, however. The static pressure probes were usually located a sufficient distance from the reflected shock wave S_r so that they were not influenced by the presence of this shock wave.[8] There is usually no problem with obtaining accurate Pitot tube measurements, even in the vicinity of oblique shock waves.[8,9] No effort was made to determine the precise orientation of the shock waves in the vicinity of the intersection T—they may have been cured there.[10]

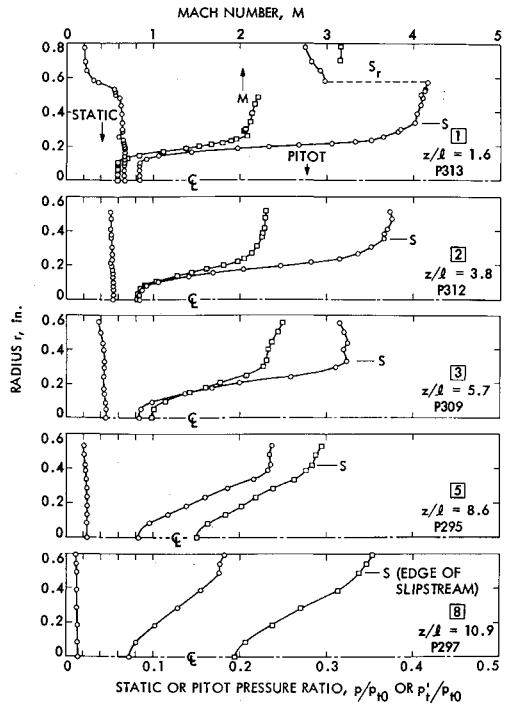

Fig. 2 Static and Pitot pressure and Mach number distributions across the flow at various axial locations.

Results

The over-all features of the centerline Mach reflection are indicated in Fig. 1 by the static pressures and Mach numbers along the centerline and along the edge of the slipstream. The flow was compressed across both the stem shock wave and the incident and reflecting shock waves to a static pressure considerably above both the upstream pressure and eventual pressure farther downstream. The core flow was then accelerated by virtue of the pressure difference and the viscous shear stress exerted at the edge of the core flow by the higher-speed flow beyond the slipstream. Along the centerline the Mach number was 0.42 just downstream of the stem shock wave. The sonic condition was located 6 shock stem heights, i.e., z/l, downstream, a location that also is in agreement with the finding of Ref. 11 in the high Mach number exhaust jet of an underexpanded nozzle flow. The flow then continued to accelerate along the centerline to a Mach number of about 2. Simultaneous acceleration occurred above the edge of the slipstream in a way such that the difference between Mach numbers along the edge of the slipstream and the centerline did not change much. Near the end of the region investigated the Mach number along the slipstream edge was about 3.4.

Information on the viscous effects in the flow appears in Fig. 2 where the measured Pitot and static pressure distributions across the flow are shown at various axial locations along with the corresponding Mach number distributions calculated for $\gamma = 1.4$. The shear layer which originated at the triple

point T grew laterally and the inner edge extended to about $\frac{1}{3}$ of a shock stem height from the centerline at the first probe station ($z/l = 1.6$) downstream of the shock stem (Fig. 1). The inner edge of the shear layer apparently intersected the centerline just downstream of the second probe position at an axial location of about 4 shock stem heights. Farther downstream the shear layer continued to increase in thickness as the outer edge of the slipstream diverged. At the last probe position ($z/l = 10.9$), the outer edge of the slipstream was about 1.4 shock stem heights from the centerline. Radial gradients of the Mach number diminished in magnitude along the flow because of the lateral growth of the shear layer.

The static pressure at the various axial locations (Fig. 2) was highest along the centerline (where the Mach number was lowest) and decreased radially outward. The compression of the flow by the shock waves was apparently relieved by the decrease in pressures both axially and radially as seen in Fig. 1. The static pressures continued to decrease radially beyond the edge of the slipstream that was established by the flattening out of the Pitot pressure measurements. Consequently, the Mach numbers increased beyond the edge of the slipstream, but the slope was less. Of note is that at the first probe position, the abrupt decrease in the Pitot pressure beyond the slipstream edge denoted by S is associated with traversing across the reflected oblique shock wave S_r (Fig. 2).

Axial velocity distributions could be calculated with a small amount of error from the Mach numbers by using the upstream stagnation temperature to calculate the static temperature and thus the speed of sound for adiabatic flow. The density could then be obtained from the equation of state $p = \rho RT$ and therefore streamlines,

$$\psi = \int_0^r \rho u r dr$$

shown in Fig. 1, could be calculated. The streamlines converged slightly in the core flow region as the gas accelerated to the sonic condition along the centerline: they then diverged as the gas accelerated in the supersonic region. It should be mentioned that temperature surveys were also made across the flow with an aspirating thermocouple probe which had a 0.010-in. tip height. However, because of the relatively small difference between the thermocouple recovery temperature and the total temperature, and some uncertainty in the probe recovery factor, temperature measurements are not shown.

The slipstream shear layer caused the sonic line (Fig. 1) to be inclined to the flow rather than perpendicular to the flow as it would have been if the flow were inviscid. For an inviscid flow, there is a step change in velocity across the slipstream. Even though the viscous shear stress contributed to the acceleration of the subsonic core flow, the dominant accelerating mechanism was the pressure gradient. This behavior was deduced by comparing the axial location on the centerline location at which sonic velocity would have occurred for an isentropic expansion to the measured static pressure. In Fig. 1, it is evident that these locations are very close to each other. The location of the actual sonic velocity is farther downstream because the entropy increase in the real flow associated with viscous effects requires the flow to expand to a lower pressure to acquire the same kinetic energy and thus Mach number as for an isentropic flow.

The measurements indicate a more rapid growth of the shear layer in subsonic flow than in supersonic flow. This difference might be expected since turbulent intensities are higher in subsonic than supersonic flows, and therefore the growth of the shear layer $db/dz \alpha v'/u$ should be larger in the subsonic region. The flow was, of course, being accelerated — the small amount of information that is available only for a low-speed flow indicates that v'/u decreases in an accelerating flow.[12] It is evident in Fig. 1 that the edge of the shear layer on the subsonic side did not grow linearly from the shock intersection.

References

[1] Back, L. H., Cuffel, R. F., and Massier, P. F., *Experimental Convective Heat Transfer and Pressure Distributions and Boundary Layer Thicknesses in Turbulent Flow Through a Variable Cross-Sectional Area Channel*, 4th International Heat Transfer Conference, Paris-Versailles, 1970, Vol. II, FC 2.1, Elsevier, Amsterdam.

[2] Adamson, T. C., Jr., "The Structure of the Rocket Exhaust Plume Without Reaction at Various Altitudes," *Supersonic Flow, Chemical Processes and Radiation Transfer*, edited by D. B. Olfe and V. Zakkay, Pergamon Press, New York, 1964, pp. 177–200.

[3] Fraser, R. P., Rowe, P. N., and Coulter, M. O., "Efficiency of Supersonic Nozzles for Rockets and Some Unusual Designs," *Proceedings of the Institution of Mechanical Engineers*, Vol. 171, No. 16, 1957, pp. 553–580.

[4] Fraser, R. P., Eisenklam, P., and Wilkie, D., "Investigation of Supersonic Flow Separation in Nozzles," *Journal of Mechanical Engineering Science*, Vol. 1, No. 3, 1959, pp. 267–279.

[5] Back, L. H., Massier, P. F., and Cuffel, R. F., "Heat Transfer Measurements in the Shock-Induced Flow Separation Region in a Supersonic Nozzle," *AIAA Journal*, Vol. 6, No. 5, May 1968, pp. 923–925.

[6] Nagamatsu, H. T. and Horvay, G., "Supersonic Jet Noise," AIAA Paper 70-237, New York, 1970.

[7] Cronvich, L. L., "Pressure Distributions Over a Cylinder With Conical or Hemispherical Head at Supersonic Velocities," Rept. CM-528, Feb. 1949, Applied Physics Lab., Johns Hopkins Univ., Silver Spring, Md.; also Shapiro, A. H., *The Dynamics and Thermodynamics of Compressible Fluid Flow*, Vol. II, Ronald Press, New York, 1954, pp. 696–697.

[8] Back, L. H. and Cuffel, R. F., "Static Pressure Measurements Near an Oblique Shock Wave," *AIAA Journal*, Vol. 9, No. 2, Feb., 1971, pp. 345–347.

[9] Bannink, W. J. and Nebbeling, C., "Determination of the Position of a Shock Wave from Pitot Tube Experiments," *AIAA Journal*, Vol. 7, No. 4, April 1969, pp. 796–797.

[10] Sternberg, J., "Triple Shock-Wave Intersections," *The Physics of Fluids*, Vol. 2, No. 2, March-April 1959, pp. 179–206.

[11] Bowyer, J., D'Attorre, L., and Yoshihara, H., "The Flow Field Resulting from Mach Reflection of a Convergent Conical Shock at the Axis of a Supersonic, Axially Symmetric Jet," GDA 63-0586, July 1963, General Dynamics/Astronautics Space Science Lab., San Diego, Calif.; also AD 463487.

[12] Uberoi, M. S., "Effect of Wind-Tunnel Contraction on Free-Stream Turbulence," *Journal of the Aeronautical Sciences*, Vol. 23, No. 8, 1956, pp. 754–764.